Isothermal Cold Crystallization Kinetics of Polylactide/Nucleating Agents

Ruogu Liao, Bin Yang, Wei Yu, Chixing Zhou

Department of Polymer Science and Engineering, Shanghai Jiao Tong University, People's Republic Of China

Received 1 August 2006; revised 27 October 2006; accepted 3 November 2006
DOI 10.1002/app.25733
Published online in Wiley InterScience (www.interscience.wiley.com).

ABSTRACT: The isothermal cold crystallization kinetics of polylactide (PLA)/nucleating agents ($CaCO_3$, TiO_2, and $BaSO_4$, content from 0.5–2.0 wt %) was investigated by differential scanning calorimetry in the temperature range of 120–124°C. With blending nucleating agents, the crystallinity of PLA had a maximum crystallinity of 14.9%. Crystallization rate decreased with increasing crystallization temperature in the researched content range. The crystallization rate followed the Avrami equation with the exponent n around 4.5. From Lauritzen–Hoffman equation, the nucleation parameter K_g was estimated. And from the value of K_g, regime II crystallization behavior can be concluded. Then the lateral and fold surface free energy were calculated from K_g. © 2007 Wiley Periodicals, Inc. J Appl Polym Sci 104: 310–317, 2007

Key words: crystallization; nucleation; differential scanning calorimetry (DSC)

INTRODUCTION

In recent years, much attention has been focused on biodegradable and biocompatible polymers. In this direction, polylactide (PLA) is one of the most promising candidates. PLA has good mechanical properties, thermal plasticity, and is readily fabricated, thus being a promising polymer for various end-use applications.[1,2] The most common synthetic route to PLA is the ring-opening polymerization of lactide, the cyclic dimer of lactide acid. The lactide monomer can be derived from renewable agricultural sources, and relatively low cost monomer production has generated industrial interest in large volume production of fibers and films.

The physical and mechanical properties of crystallizable PLA are largely dependent on its solid-state morphology and level of crystallinity, while the crystallinity of PLA is influenced deeply by its composition.[3–5] Schmidt and Hillmyer[3] found that the addition of poly(D-lactide) (PDLA) into poly(L-lactide) (PLLA) led to the reduction in the overall extent of PLLA crystallization. Baratian et al.[5] also found that with increasing the content of D-lactide, crystallinity and spherulite growth rate decreased substantially.

Understanding of crystallization kinetics is also important because the control of crystallization factors allows for the design of materials with desirable properties. In recent years, there were some papers on the crystallization kinetics of PLA.[6–14] Lorenzo[6] measured spherulite growth rate of PLLA from melt by isothermal and nonisothermal methods and detected a regime II-III transition at 120°C. Abe[10] found that the regime transitions of PLA crystal growth, from regime III to regime II and from regime II to regime I, occurred at around 120 and 147°C, respectively, while Iannace[9] found the transition from regime II to regime III was presented around 115°C. The cold crystallization of PLLA was studied by Mano et al.[7] By means of simultaneous SAXS and WAXS, they found that the crystallization rate of PLLA decreased with increasing molecular weight. Miyata and Masuko[8] studied the effect of molecular weight on the crystallization characters of PLLA too. Composition also had an effect on the crystallization rate.[11,12]

Although PLA possesses many desirable properties, its crystallization rate is extremely slow in comparison with commercial thermoplastics. The most viable method to increase the overall crystallization rate was the blending of nucleating agent. Relatively few studies had focused on the nucleating agents for PLA. Clay was used by Okamoto and coworkers[15] who found that the overall crystallization rate and spherulitic texture of PLA were strongly influenced by montmorillonite particles. At the same time they found that blending of low-molecular weight aliphatic acid also increased the crystallization rate.[16] Anderson et al.[3,11,17,18] compared the nucleation efficiency of sterocomplex crystallites and the common nucleating agent talc. It was found that with 6 wt % talc, the crystallization half-time ($t_{1/2}$) of PLA at

Correspondence to: C. Zhou (cxzhou@sjtu.edu.cn).
Contract grant sponsor: Natural Science Foundation of China; contract grant numbers: 10590355, 50390095.

Journal of Applied Polymer Science, Vol. 104, 310–317 (2007)

TABLE I
Sample Name and Its Composition

Sample	PLA	$BaSO_4$	$CaCO_3$	TiO_2
PLA-B5	99.5	0.5	–	–
PLA-C5	99.5	–	0.5	–
PLA-T5	99.5	–	–	0.5
PLA-T10	99.0	–	–	1.0
PLA-T15	98.5	–	–	1.5
PLA-T20	98.0	–	–	2.0

120°C was <1 min but sterocomplex crystallites were even more effective. Hiltner and coworkers[19,20] and Pluta[21] believed that blending of poly(ethylene glycol) (PEG) accelerated crystallization of PLA and decreasing the amount of PEG in the blend decreased the crystallization rate of PLA. Some other fillers (such as $CaCO_3$, hydroxyapatite, calcium hydrogen phosphate, bioactive glass) were also investigated,[22–27] but only for mechanical properties.

Although there were some papers on the crystallization kinetics and nucleating agents, there were few papers on the research of kinetics of PLA/nucleating agent system. In this article, three nucleating agents ($CaCO_3$, TiO_2, and $BaSO_4$) were blended with industrial produced PLA whose crystallinity was very low. After adding nucleating agents, the crystallinity of PLA increased. By DSC technique, the isothermal cold crystallization kinetics was studied. The Avrami exponent (n), crystallization rate constant (k), nucleation parameter (K_g), and folding surface free energy (σ_e) were obtained from DSC data. In the temperature range of 120–124°C, the crystallization rate decreased with increasing crystallization temperature. From the value of K_g, the crystallization behavior of regime II was concluded and values of σ_e were in agreement with that reported in other literatures.

EXPERIMENTAL

Materials and preparation

PLA was NatureWorks product 3051D whose specific gravity and melt index were 1.24 and 10–30g/10 min (190°C), respectively. The content of L-lactide was about 96 wt % and the monomer was less than 0.3 wt %. The sample was used as received without further treatment. Nano-$CaCO_3$ (YH-306) was a commercial product of Shanghai Yaohua nanotechnique, China. Its diameter was less than 100 nm and surface modified by aliphatic acid. Nano-$BaSO_4$ (AY-2) was provided by Shanghai Anyi nanomaterial, and nano-TiO_2 (CYU-103) was from Shanghai Shanghui nanotechnique, China.

PLA was dried at 50°C for 9 h and nucleating agents were dried at 105°C for 6 h under vacuum before mixing. PLA/nucleating agent composites were prepared by direct melt mixing nucleating agents with PLA in a Rheomix-600 mixer (Haake Rheocord 900, Germany) at 180°C and 60 rpm for 8 min, and nucleating agent content varied form 0.5 wt % to 2.0 wt %, respectively. The detailed compositions are listed in Table I.

Differential scanning calorimetry (DSC) analysis

A Perkin-Elmer PYRIS 1 DSC was used to study the thermal properties (such as T_g and T_m) and isothermal cold crystallization behavior of PLA. A sample of about 5 mg was first heated from 20 to 180°C at 10°C/min and hold for 5 min to erase the thermal history, and then it was cooled at the same speed to 20°C and held for another 5 min. Finally, the sample was scanned again to 180°C at 10°C/min to get T_g and T_m. Different heating and cooling rates from 2.5 to 40°C/min were also performed. Isothermal cold crystallization was performed as follow. The sample was heated from 20 to 180°C at 150°C/min and held for 5 min to destroy the crystal of PLA. Then it was cooled to 20°C at 150°C/min and held for another 5 min. Finally, it was heated at the same speed to a certain crystallization temperature (120–124°C in this article) and held until the crystallization finished, then heated at 10°C/min to 180°C again to get the melt temperature.

RESULTS AND DISCUSSION

Thermal properties analysis

Figure 1 showed the thermal behavior of PLA-T5 at a scanning rate of 10°C/min. It can be seen that the two heating curves are almost the same. The T_g was about 58°C and both the curves had an exothermic peak (cold crystallization, at about 125°C) and an endothermic peak (melting of crystallization, at about 150°C), while there was no crystallization peak on the cooling

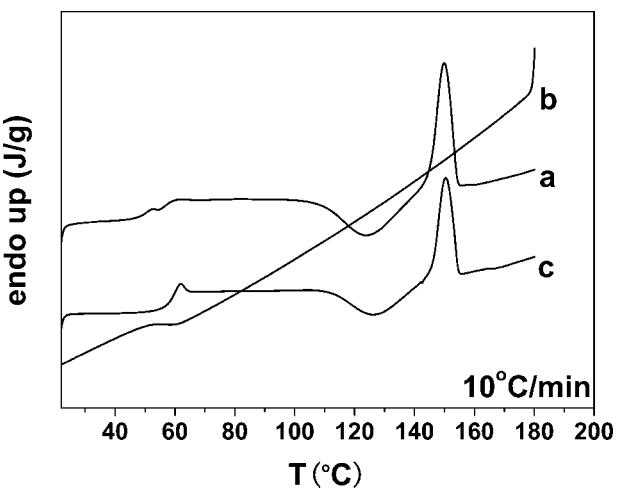

Figure 1 Thermal analysis of PLA-T5 at a scanning rate of 10°C/min (a) first heating curve; (b) cooling curve; (c) second heating curve.

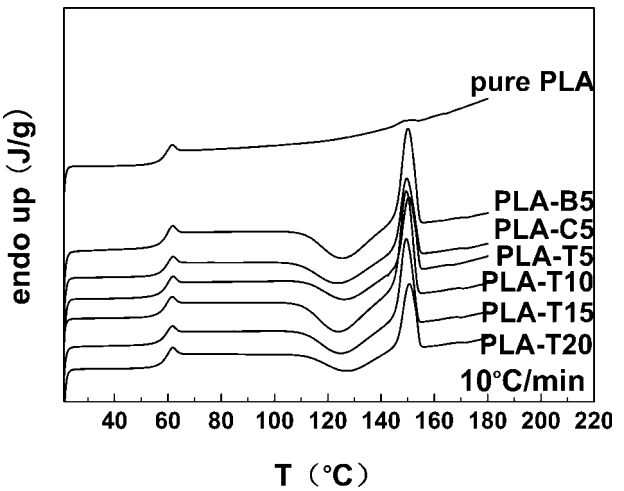

Figure 2 The second heating curves of pure PLA and PLA/nucleating agent system.

curve. It seemed that in the process of cooling there was no crystallization. But from the DSC curve of pure PLA in Figure 2, there was a little endothermic peak that corresponded to crystallinity of 5.6 wt %. The cooling curve of it also had no crystallization peak and there was no exothermic peak on the second heating curve. So it was believed that there was crystallization in the course of cooling but the crystallization peak was hidden by the lengthy cooling process. This was the reason that cold crystallization kinetics research was performed. Figure 2 was the second heating curves of pure PLA and PLA/nucleating agent system. The data obtained from Figure 2 were listed in Table II. It can be seen that there was just a little endothermic peak on the curve of pure PLA, and the crystallinity was about 5.6 wt %. After adding nucleating agents, an exothermic peak appeared on the heating curve. It can be concluded that in the course of heating more crystal was formed. So the crystallinity of PLA increased. The sample blended with 0.5 wt % $BaSO_4$ had the highest crystallinity while that blended with $CaCO_3$ had the lowest crystallinity. Because the diameter of all the nucleating agents was almost the same (about 100 nm), and the surface was treated by aliphatic acid, the difference in crystallinity may be the result of different nucleating agent shape[29] and property. The shape of $CaCO_3$ was cubic, while the other two were spherical. It seemed that $BaSO_4$ was more effective for the crystallization of PLA in this experiment. With increasing content of nucleating agent, the crystallinity was decreasing, which can be seen from PLA/TiO_2 system. It can be said that a little amount of nucleating agent helped form the polymer crystal while higher nucleating agent content hindered the ordered arrangement of molecular chain and resulted in low crystallinity. To confirm that crystal can not form was not because of the heating rate, the sample was scanned at different rates (Fig. 3). It was found that when heating rate was higher than 20°C/min, there was no endothermic peak on the curves. When scanned at 2.5°C/min, two endothermic peaks appeared. It was thought that when the scan rate was slow, there was enough time for the thinner crystals to melt and then to recrystallize before giving a second endotherm at a higher temperature.[30]

Isothermal cold crystallization kinetics from Avrami analysis

Isothermal cold crystallization was studied by the quenched amorphous glass being heated rapidly to the T_c (crystallization temperature). The isothermal crystallization kinetics can be better visualized by evaluating the degree of crystalline conversion as a function of time at a constant temperature. The relative crystallinity at different crystallization time, X_t, can be calculated according to the equation:

$$X_t = Q_t/Q_\infty = \frac{\int_0^t (dH/dt)dt}{\int_0^\infty (dH/dt)dt} \quad (1)$$

where Q_t and Q_∞ is the heat generated at time t and infinite time, respectively, and dH/dt is the rate of heat evolution.

Relative crystallinity had been plotted in Figure 4 with crystallization time. From Figure 4(a), it was found that with increasing crystallization tempera-

TABLE II
Parameters Obtained From Second Scan of DSC Curves

Sample	T_g (°C)	T_c (°C)	T_m (°C)	$-\Delta H_c$ (J/g)	ΔH_m (J/g)	X_c (%)[a]
Pure PLA	57.7	–	148.6	–	5.21	5.6
PLA-B5	58.0	124.3	150.0	8.4	22.4	14.9
PLA-C5	58.3	124.1	149.6	12.9	19.9	7.5
PLA-T5	58.2	126.1	150.5	7.6	17.9	10.9
PLA-T10	58.6	124.4	149.9	13.2	22.3	9.7
PLA-T15	58.1	124.5	149.5	12.4	21.4	9.6
PLA-T20	58.2	126.3	150.6	6.6	15.4	9.4

[a] $X_c(\%) = 100 \times (\Delta H_c + \Delta H_m)/\Delta H_m^0$, $\Delta H_m^0 = 93.7 J/g$.[28]

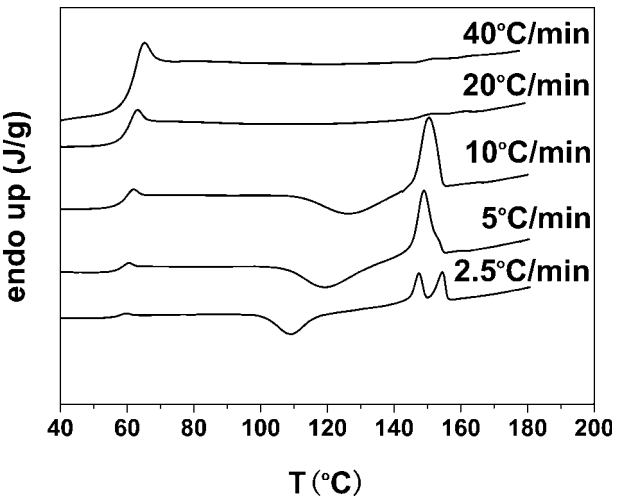

Figure 3 The second heating curves of PLA-T5 at different scanning rate.

ture the relative crystallinity was decreasing at a certain crystallization time, which meant that the crystallization rate was decreasing. Increasing crystallization temperature, the rate of nucleation decreased, and then the overall crystallization rate was decreasing. As for different nucleating agents, it can be seen from Figure 4(b) that PLA/$CaCO_3$ sample had the fastest crystallization rate at 120°C. In the system of PLA/TiO_2, when the content of TiO_2 was 1 wt %, the sample had the fastest crystallization rate.

The theory of Avrami is used to analyze the increase of relative crystallinity with time:

$$X_t = 1 - \exp(-kt^n) \tag{2}$$

$$\log[-\ln(1 - X_t)] = \log k + n \log t \tag{3}$$

where k is the crystallization rate constant and n is Avrami exponent whose value depends on the mechanism of nucleation and on the form of crystal growth. Accordingly, the Avrami exponent n and crystallization rate k can be obtained from the slope and intercept, respectively, in a plot of log[-ln(1 − X_t)] versus log$t$, as shown in Figure 5. For the isothermal crystallization, a linear portion of about 30–70% relative crystallinity was used to obtain n and k. Figure 5 was the plots of log[-ln(1 − X_t)] versus log$t$ for isothermal crystallization of PLA/nucleating agents. The data from the plots and Avrami equation were listed in Table III. The Avrami exponents obtained were very close, in the range of 4–5. It implied that the crystals in the PLA/nucleating agent systems showed heterogeneous nucleation and spherulitic growth[12] or grain like morphology[31] (3-D growth that can be confirmed by polarized light microscopy[31]) under the experimental condition. The values of n reported in literatures were in the range of 2–5.4[7,9,12,13,18,32] depending on

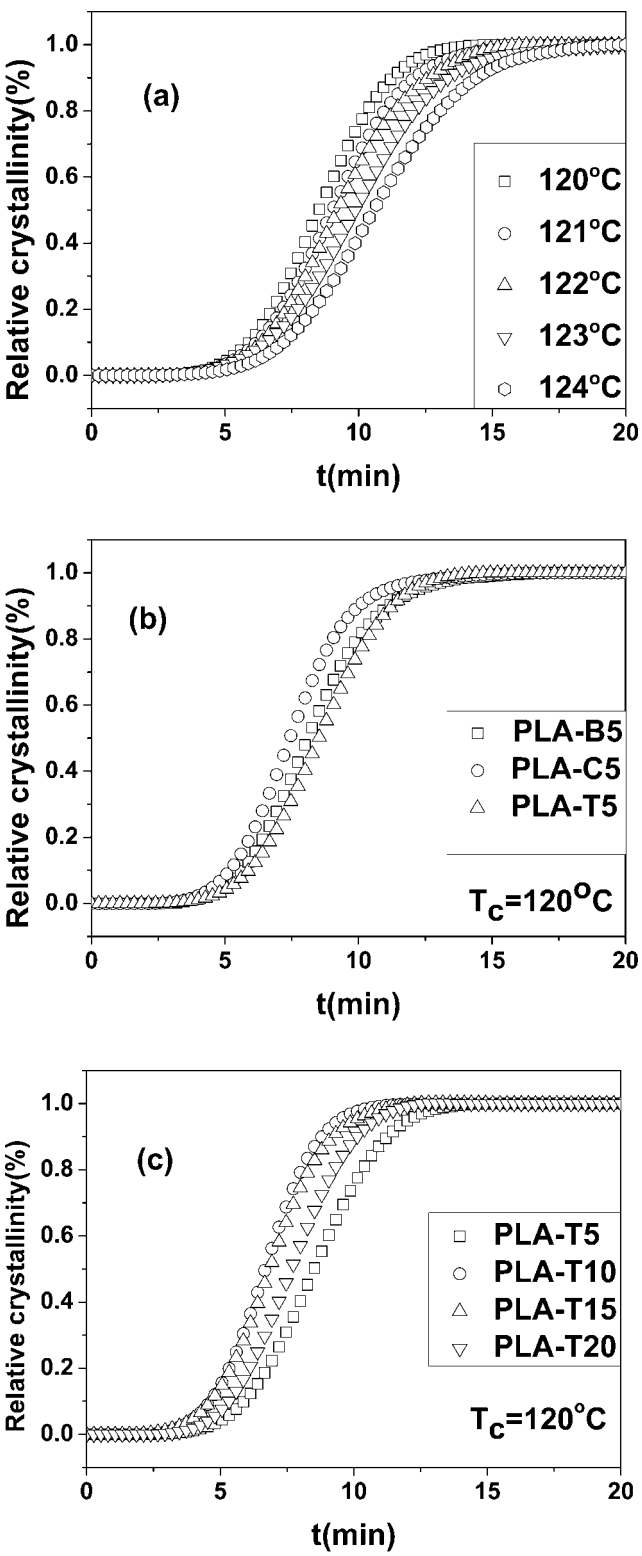

Figure 4 Relative crystallinity X_t versus crystallization time t curves of different crystallization temperature, type of nucleating agent and content of nucleating agent (a) PLA-T5 crystallized at different temperature; (b) different PLA/nucleating agents crystallized at 120°C; (c) different content of PLA/TiO_2 crystallized at 120°C.

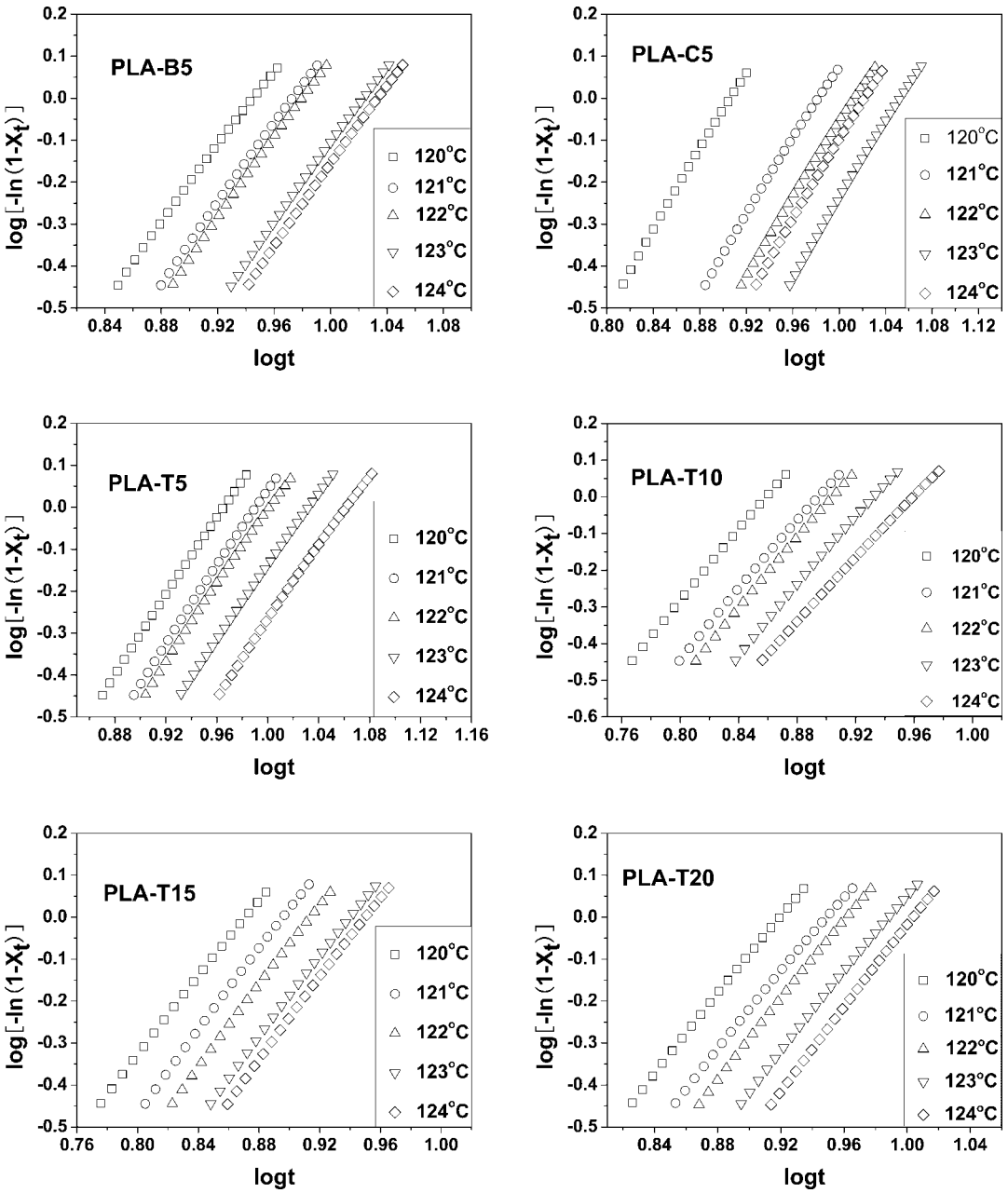

Figure 5 Plots of log[-ln(1-*X*t)] versus log*t* for isothermal crystallization of PLA/nucleating agents.

the mechanism of nucleation, the form of crystal growth and the detecting techniques used (such as DSC, WAXS, FTIR etc.). The values here may be the result of a change of the nucleation mechanism toward a more sporadic nucleation that nuclei generation had greater time dependence[33] or a thermal nucleation process.[34]

Crystallization half-time, $t_{1/2}$, is defined as the time at which the extent of crystallization reaches 50%. It is also regarded as a very important crystallization kinetics parameter. Usually it is employed to characterize the crystallization rate directly. It can be said that the longer the crystallization half-time, the slower the crystallization rate. Furthermore, from n and k, $t_{1/2}$ can be obtained from eq. (4):

$$t_{1/2} = \left(\frac{\ln 2}{k}\right)^{1/n} \tag{4}$$

As can be seen in Table III, the crystallization half-time increased with the increasing of crystallization temperature under our experimental conditions, which meant slower crystallization rate. The results in Table III were in accordance with those deduced from Figure 4. Usually, the rate of crystallization, G, is described as the reciprocal of $t_{1/2}$ i.e., $(t_{1/2})^{-1}$.

TABLE III
Kinetics Parameters Obtained From Isothermal Cold Crystallization Experiments and Avrami Analysis

Sample	T_c (°C)	n	K (min^{-n}) $\times 10^5$	$t_{1/2}$ (min)	$(t_{1/2})^{-1}$ $(\text{min})^{-1}$
PLA–B5	120	4.58	4.79	8.10	0.123
	121	4.73	2.51	8.69	0.115
	122	4.79	2.04	8.83	0.113
	123	4.70	1.55	9.76	0.102
	124	4.95	1.12	10.01	0.100
PLA–C5	120	4.73	5.13	7.47	0.134
	121	4.50	3.89	8.80	0.114
	122	4.50	2.75	9.51	0.105
	123	4.61	1.41	10.42	0.096
	124	4.69	1.62	9.72	0.103
PLA–T5	120	4.65	3.23	8.54	0.117
	121	4.62	2.69	9.01	0.111
	122	4.51	3.09	9.22	0.108
	123	4.39	2.95	9.90	0.101
	124	4.39	2.19	10.60	0.094
PLA–T10	120	4.83	7.24	6.67	0.150
	121	4.63	7.24	7.24	0.138
	122	4.73	5.25	7.43	0.134
	123	4.64	4.79	7.88	0.127
	124	4.28	7.94	8.33	0.120
PLA–T15	120	4.62	9.55	6.85	0.146
	121	4.85	4.57	7.29	0.137
	122	4.83	3.89	7.59	0.132
	123	4.79	3.16	8.06	0.124
	124	4.86	2.45	8.24	0.121
PLA–T20	120	4.69	4.90	7.67	0.130
	121	4.56	4.47	8.21	0.122
	122	4.73	2.82	8.48	0.118
	123	4.68	2.34	9.02	0.111
	124	4.93	1.10	9.36	0.107

The calculated values of $(t_{1/2})^{-1}$ were also listed in Table III.

Equilibrium melting point

According to the theoretical consideration by Hoffman and Weeks, the equilibrium melting point temperature can be obtained by the intersection of the resulting straight line with the line $T_m = T_c$, and the dependence of the T_m on the T_c is given by

$$T_m = T_m^0\left(1 - \frac{1}{2\beta}\right) + \frac{1}{2\beta}T_c \quad (5)$$

where T_m^0 is the equilibrium melting point and β describes the growth of lamellar thickness during crystallization. Under equilibrium conditions, β equals 1. The equilibrium melting point obtained from Figure 6 was equal to 165.8°C that was lower than the values (169–227°C) reported in other literatures.[4,6,8–12,15,32,35] And the values reported in these literatures were also different from each other. This was mainly attributed to the different composition of PLA in these literatures. On the other hand, different detecting techniques and treatment methods can also contribute to the different values. As for the value in this article, it also may be because the adding of nucleating agent attenuated the crystal and correspondingly decreased the thickness of crystal lamella.

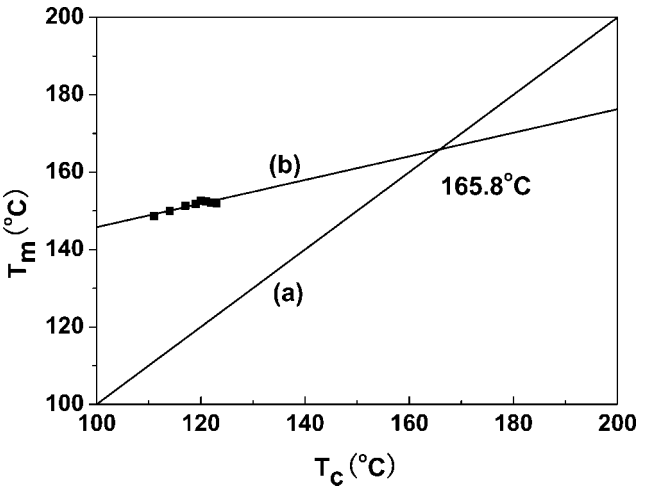

Figure 6 Determination of equilibrium melting point by Hoffman–Weeks equation (a) curve of $T_m = T_c$; (b) linear fit curve of T_m corresponding to each T_c.

Nucleation parameter

The Lauritzen–Hoffman equation[36] is employed to analyze the spherulitic growth rate G of PLA:

$$G = G_0 \exp[-U^*/R(T_c - T_\infty)] \exp[-K_g/T_c \cdot \Delta T \cdot f] \quad (6)$$

where K_g is the nucleation parameter, T_c is the crystallization temperature, ΔT is supercooling $T_m^0 - T_c$, where T_m^0 is the equilibrium melt temperature, f is the correction factor defined as $2T_c/(T_m^0 + T_c)$ that account for the change in heat of fusion as the tempera-

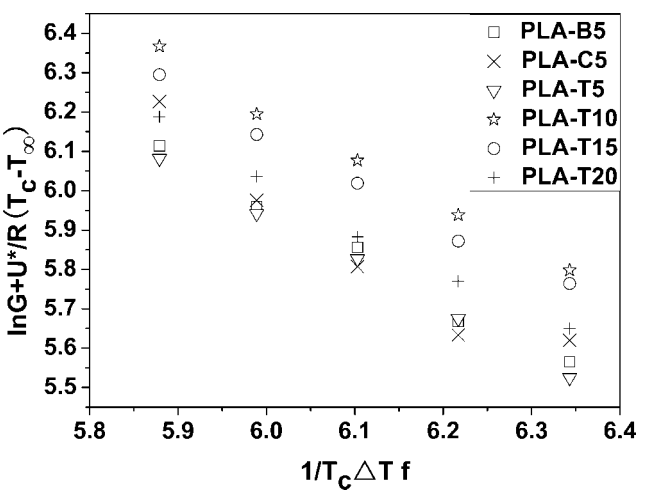

Figure 7 Plots of $\ln G + U^*/R(T_c - T_\infty)$ versus $1/T_c\Delta T f$ for different PLA/nucleating agent system.

TABLE IV
Calculated Values of K_g, $\sigma\sigma_e$, and σ_e by Lauritzen–Hoffman Equation and Equation 7

	PLA-B5	PLA-C5	PLA-T5	PLA-T10	PLA-T15	PLA-T20
K_g (K^2)/10^5	1.30	1.36	1.19	1.21	1.15	1.16
$\sigma\sigma_e$ (erg^2/cm^4)	688	720	630	640	609	614
σ_e (erg/cm^2)	74.8	78.3	68.5	70.0	66.2	66.7

ture is decreased below T_m^0, U^* is the activation energy for transportation of segments to the crystallization site whose value is 6280 J/mol, R is the gas constant, T_∞ is the hypothetical temperature where all motion associated with viscous flow ceases, which is expressed as T_g-30 K, and G_0 is the front constant. In this equation, the first exponential controls the rate variations occurring at high degree of undercooling, while the second exponential accounts for the driving force of crystallization and contains thermodynamic characteristics such as side and fold surface free energy. Using a theoretical approach, it can be shown that the spherulitic growth rate G can be considered proportional to $(t_{1/2})^{-1}$. So Eq. (6) can be written as Eq. (7).[9] This method was also used in many other literatures.[34,37,38]

$$\left(\frac{1}{t_{1/2}}\right) = \left(\frac{1}{t_{1/2}}\right)_0 \exp[-U^*/R(T_c - T_\infty)] \times \exp\left[-K_g/T_c \cdot \Delta T \cdot f\right] \quad (7)$$

There are three types of crystallization behaviors (regimes I, II, III). Crystallization rate is a function of the rate, i, at which the nucleus is formed and of the rate, g, with which the surface nucleus spreads on the crystal surface. When $i < g$, regime I type of crystallization occurs. When $i \approx g$, it crystallizes by the regime II. The regime III type is a case where i is much higher than g. The nucleation parameter K_g depends on the crystallization regime and is defined as[36]

$$K_g = \frac{n_i b \sigma \sigma_e T_m^0}{k \Delta H} \quad (8)$$

where b is the layer thickness, σ and σ_e are lateral surface free energy and fold surface free energy respectively. ΔH is the heat of fusion per unit volume, and k is Boltzmann constant. The value of n_i is depending on the regime of crystallization and it is theoretically given as 4 for regime III and 2 for II respectively.

When plotting $\ln G + U^*/R(T_c\text{-}T_\infty)$ with $1/T_c\Delta Tf$ (Fig. 7), the value of K_g can be obtained from the slope. The values of K_g obtained from the plots were listed in Table IV. The values of K_g obtained were somewhat lower than the values reported in literatures,[4,6,11,31] most of which were in the range of 1.8–2.5 $\times$ 10^5 K^2. In the process of data treatment, it was found that the value of T_m^0 influenced the slope i.e., K_g value, notably. Because the equilibrium melting point used here (165.8°C) was lower than the values (169–227°C) reported in literature, it was acceptable to get a lower K_g value. At the same time, Mo[37] found that the value of K_g got from cold crystallization was lower than that got from melt crystallization of poly (aryl ether ketone ether ketone ketone) (PEKEKK). So the value obtained here was reasonable. It was believed that the values in this range belonged to the behavior of regime II. Tsuji,[4] Lorenzo,[6] and Abe[10] found that the regime transition of PLA crystal growth, from regime III to regime II, occurred at around 120°C. So it can be concluded that the crystallization behavior of PLA/nucleating agent system under experimental condition belonged to regime II.

The Kg values are used to calculate the fold surface free energy according to Eq. (8). The lateral surface free energy is determined by the Thomas–Stavely equation[8] $\sigma = 0.1 \cdot \Delta h_f b$. Using the literature values of $\Delta h_f = 1.74 \times 10^8$ J/m^3 and $b = 0.517$ nm, the value of σ was 9.2 erg/cm^2. The values of σ_e obtained were listed in Table IV. These values were in well agreement with values in other literatures.[5,8]

CONCLUSIONS

The isothermal cold crystallization kinetics of PLA/nucleating agents was studied by DSC. Three nucleating agents ($CaCO_3$, TiO_2, and $BaSO_4$, content from 0.5–2.0 wt %) were blended with PLA. After blending a little amount of nucleating agent, the crystallinity of PLA increased. The maximum crystallinity (14.9%) occurred when 0.5 wt % $BaSO_4$ was added into PLA. In the experimental temperature range, the crystallization rate was decreasing with the increasing of crystallization temperature which can be seen from the PLA/TiO_2 system. When the content of nucleating agent was 0.5 wt %, the system had the highest crystallinity. So nucleating agent $BaSO_4$ and TiO_2 had better effects on the crystallinity. When the content of nucleating agent was 1 wt % and crystallized at 120°C, the system had higher crystallinity and highest crystallization rate. The overall crystallization rate followed the Avrami equation with the exponent n around 4.5 that indicated a 3-D growth.

The nucleation parameter was determined by Lauritzen–Hoffman equation. From the values of K_g and the crystallization temperature, it can be concluded that the crystallization behavior of PLA/nucleating

agent system belonged to regime II under experimental condition. The lateral and fold surface free energy were also calculated from K_g and Thomas–Stavely equation. The values of fold surface free energy obtained here were in the range of 66–78 erg/cm^2 which was in agreement with the values reported in other literatures.

References

1. Tsuji, H.; Ikada, Y. J Appl Polym Sci 1998, 67, 405.
2. Martin, O.; Averous, L. Polymer 2001, 42, 6209.
3. Schmidt, S. C.; Hillmyer, M. A. J Polym Sci Part B: Polym Phys 2001, 39, 300.
4. Tsuji, H.; Miyase, T.; Tezuka, Y.; Saha, S. K. Biomacromolecules 2005, 6, 244.
5. Baratian, S.; Hall, E. S.; Lin, J. S.; Xu, R.; Runt, J. Macromolecules 2001, 34, 4857.
6. Lorenzo, M. L. D. Polymer 2001, 42, 9441.
7. Mano, J. F.; Wang, Y. M.; Viana, J. C.; Denchev, Z.; Oliveira, M. J Macromol Mater Eng 2004, 289, 910.
8. Miyata, T.; Masuko, T. Polymer 1998, 39, 5515.
9. Iannace, S.; Nicolais, L. J Appl Polym Sci 1997, 64, 911.
10. Abe, H.; Kikkawa, Y.; Inoue, Y.; Doi, Y. Biomacromolecules 2001, 2, 1007.
11. Tsuji, H.; Tezuka, Y. Biomacromolecules 2004, 5, 1181.
12. Kolstad, J. F. J Appl Polym Sci 1996, 62, 1079.
13. Zhang, J.; Tsuji, H.; Noda, I.; Ozaki, Y. Macromolecules 2004, 37, 6433.
14. Kikkawa, Y.; Abe, H.; Iwata, T.; Inoue, Y.; Doi, Y. Biomacromolecules 2001, 2, 940.
15. Nam, J. Y.; Ray, S. S.; Okamoto, M. Macromolecules 2003, 36, 7126.
16. Nam, J. Y.; Okamoto, M.; Okamoto, H.; Nakano, M.; Usuki, A.; Matsuda, M. Polymer 2006, 47, 1340.
17. Yamane, H.; Sasai, K. Polymer 2003, 44, 2569.
18. Anderson, K. S.; Hillmyer, M. A. Polymer 2006, 47, 2030.
19. Hu, Y.; Hu, Y. S.; Topolkaraev, V.; Hiltner, A.; Baer, E. Polymer 2003, 44, 5681.
20. Wang, Z.; Wang, X.; Hsiao, B. S.; Andjelic, S.; Jamiolkowski, D.; Mcdivitt, J.; Fischer, J.; Zhou, J.; Han, C. C. Polymer 2001, 42, 8965.
21. Pluta, M. Polymer 2004, 45, 8239.
22. Urayama, H.; Ma, C.; Kimura, Y. Macromol Mater Eng 2003, 288, 562.
23. Hong, Z.; Zhang, P.; He, C.; Qiu, X.; Liu, A.; Chen, L.; Chen, X.; Jing, X. Biomaterials 2005, 26, 6296.
24. Vogt, S.; Kuhn, K.-D.; Ege, W.; Pawlik, K.; Schnabelrauch, M. Mat-wiss u Werkstofftech 2003, 34, 1041.
25. Maquet, V.; Boccaccini, A. R.; Pravata, L.; Notingher, I.; Jerome, R. Biomaterials 2004, 25, 4185.
26. Bleach, N. C.; Nazhat, N. S.; Tanner, K. E.; Kellomaki, M.; Tornala, P. Biomaterials 2002, 23, 1579.
27. Bleach, N. C.; Tanner, K. E.; Kellomaki, M.; Tornala, P. J Mater Sci: Mater Med 2001, 12, 911.
28. Liu, H.; Hsieh, C. T.; Hu, D. S. G. Polym Bull 1994, 32, 463.
29. Lyu, S. G.; Park, S.; Sur, G. S. Korean J Chem Eng 1999, 16, 538.
30. Sarasua, J.; Prud'homme, R. E.; Wisniewski, M.; Borgne, A. L.; Spassky, N. Macromolecules 1998, 31, 3895.
31. Mijovic, J.; Sy, J.-W. Macromolecules 2002, 35, 6370.
32. Cho, J.; Baratian, S.; Kim, J.; Yeh, F.; Hsiao, B. S.; Runt, J. Polymer 2003, 44, 711.
33. Chisholm, B. J.; Zimmer, J. G. J Appl Polym Sci 2000, 76, 1296.
34. Liu, T.; Mo, Z.; Wang, S.; Zhang, H.; Wang, J.; Na, H.; Wu, Z. J Appl Polym Sci 1997, 64, 1451.
35. Huang, J.; Lisowski, M. S.; Runt, J.; Hall, E. S.; Kean, E. S.; Buehler, N. Macromolecules 1998, 31, 2593.
36. Hoffman, J. D.; Miller, R. L. Polymer 1997, 38, 3151.
37. Qiu, Z.; Mo, Z.; Zhang, H.; Sheng, S.; Song, C. J Polym Sci B: Polym Phys 2000, 38, 1992.
38. Liu, T.; Mo, Z.; Wang, S.; Zhang, H. Eur Polym J 1997, 33, 1405.